Synthesis of Agarose-*graft*-Hyaluronan Copolymer and Its Potential Application as a Peptide Carrier

Jian-Yan Huang, Lei Bao, Xuan Mao, Shun-Qing Tang

Biomedical Engineering Institute, Jinan University, Guangzhou 510632, People's Republic of China

Received 18 May 2008; accepted 10 February 2010
DOI 10.1002/app.32268
Published online 12 May 2010 in Wiley InterScience (www.interscience.wiley.com).

ABSTRACT: A novel water-soluble copolymer, agarose-*graft*-hyaluronan (Ag-*g*-HA), was synthesized as a peptide carrier, and selected properties were evaluated. In brief, agarose was degraded by hydrogen peroxide to achieve agarose with a low gelling temperature and a low molecular weight, activated by epichlorohydrin, and grafted with hyaluronic acid. The IR spectrum results of the Ag-*g*-HA copolymer showed that there were specific absorption peaks of hyaluronan at 1609 cm^{-1} (C=O), which proved that hyaluronan was successfully grafted onto the agarose chain. The elemental analysis results showed that the nitrogen content of Ag-*g*-HA was 2.57%. The grafting ratio of epoxy groups was deduced to be 66.41% according to the *N* content of the copolymer. The ζ potential analysis results disclosed that Ag-*g*-HA became negative with increasing pH above 3. Ag-*g*-HA/insulin (INS) polyelectrolyte complexes were formed via electrostatic interaction at pH 3–5.4. The results of atomic force microscopy and ζ potential analyses demonstrated that Ag-*g*-HA and INS could spontaneously form microparticles with average diameters of 2–10 μm. The result of an INS-releasing experiment *in vitro* disclosed that these particles had a significant burst release effect during the initial 30 min of release at pH 1.2 or 7.4, but the release behavior was ideal in the environment of pH 6.8. The release data could be described by the Weibull equation. These results demonstrate that the Ag-*g*-HA copolymer possessed potential as a peptide carrier. © 2010 Wiley Periodicals, Inc. J Appl Polym Sci 117: 3568–3574, 2010

Key words: biomaterials; graft copolymers; water-soluble polymers

INTRODUCTION

In recent years, the large-scale planting of seaweed has drawn considerable interest for new biomedical applications.[1–3] Among all of these seaweeds, agarose has been used widely as food in Asia and as a gel-forming agent in media for cell culture or electrophoresis analysis. Agarose is a linear galactan, which is extracted from the seaweed of the Gelidium family, and is a highly hydrophilic polymer, which has special gel properties (to form particles without chemical crosslinking) and favorable biocompatibility. However, agarose has a high molecular weight and degrades slowly; in particular, it has no specific biomedical function. These properties prevent it from being applied in medicine or other fields. To extend its applications, it is necessary to modify agarose to have a high degradation rate or a low gelling temperature or to create composites with other bioactive materials for specific functions.

Correspondence to: S.-Q. Tang (tshunqt@jnu.edu.cn).
Contract grant sponsor: 863 High-Tech Plan; contract grant number: 2007AA09Z436.
Contract grant sponsor: Guangdong Technology Plan; contract grant number: 2004B10034108.
Contract grant sponsor: National "211" Project (2007).

Hyaluronic acid (HA) is a multifunctional glycosaminoglycan that forms the basis of the extracellular matrix with repeating disaccharide units of D-glucuronic acid and *N*-acetyl-D-glucosamine linked by β-1-3 and β-1-4 glycoside bonds. It can specifically react with CD44,[4] a polymorphic family of immunologically related cell surface proteoglycans and glycoproteins which normally take part in cell-cell and cell-matrix adhesion interactions, lymphocyte activation and homing, and cell migration, which makes HA an excellent targeting agent for some cells containing abundant CD44.[5–7] However, pure HA can not remain in physiological media or tissue for a long time because of its rapid degradation. Therefore, chemically modified and crosslinked HAs have been widely developed to prolong the degradation time of HA and to improve its mechanical stability *in vivo*.[8–10] An insulin (INS)-loaded HA grafted with poly(ethylene glycol) copolymer was developed by Kazuteru[11]; in this system, INS was an ideal model for a new functional copolymer as a peptide carrier.

However, to the best of our knowledge, an agarose-*graft*-hyaluronan (Ag-*g*-HA) copolymer has not been developed to date, so we synthesized an Ag-*g*-HA copolymer in this study. HA was used as one component, presenting the ionic interaction with peptide[12,13] for efficient loading and sustained release.[14,15] The aim of this study was to evaluate the potential of the Ag-*g*-HA copolymer as a peptide carrier without

chemical crosslinking. INS was used as a model peptide, and some properties of the copolymer and the INS-loaded complex were characterized.

EXPERIMENTAL

Materials

Agarose (electrophoretic grade) was purchased from Yuanju Biotechnology Co. (Shanghai, China) and had a gel strength (1%) greater than 700 g/cm^2 and a melting point of 87–89°C. HA (molecular weight = 6 kDa) was purchased from Furuida Biochemical Co. (Shandong, China). Porcine INS was obtained from Wanbang Biotech Co. (Jiangsu, China).

Synthesis of the Ag-*g*-HA copolymers

Agarose (2% w/w) was dissolved in 95°C water and cooled to 55°C; then, 30% H_2O_2 (2% v/v, Guangzhou Chemical Reagent Factory, Guangzhou, China) was used to degrade agarose. The solution was stirred and reacted at 55°C for 6 h. After the evaporation of water, the degraded agarose was precipitated three times with ethanol with a proportion of ethanol to water of 4 : 1 v/v and then lyophilized. The degraded agarose (1% w/w) was further completely dissolved by heating and cooled to 30°C, and a NaOH solution (0.5% w/w) and epichlorohydrin (4% v/v, Tianjin Chemical Reagent Factory, Tianjin, China) were added. The aqueous system was kept stirring and reacting at 30°C for 3 h [eq. (1)]. Then, the pH value of the reaction solution was adjusted to 7.0 with 0.1*M* HCl. Hence, most of the epichlorohydrin was evaporated (without heating) *in vacuo*, the solution was added with HA, and kept stirring for 48 h [eq. (2)]. The amount of the added HA was calculated according to epoxy grouping in the agarose chain. After the evaporation of water, the reaction mixture was dialyzed for 72 h with an 8–12-kDa cellulose membrane in 1000 mL of deionized water at room temperature, and deionized water was replaced once every 8 hours over 3 days. Finally, the sample was lyophilized to obtain the Ag-*g*-HA copolymer:

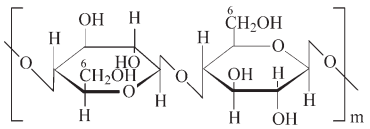

Agarose (R_6-OH)

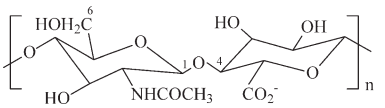

Hyaluronan (HA_6-OH)

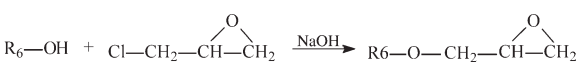

(1)

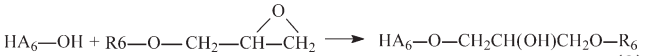

(2)

Preparation of the Ag-*g*-HA/INS complex

Ag-*g*-HA was dissolved in a 90°C sodium sulfate solution (7 mL, 1*M*) and cooled to room temperature to obtain a clear solution; then, INS was added to the solution, and a transparent gel was formed at pH 1.6 by the addition of 1.0 mL of 1*M* hydrochloric acid. The gel was dialyzed in Tris buffer (0.5 m*M*, pH 6.5, tris(hydroxymethyl)methylamine, Guangzhou Chemical Reagent Factory) for 48 h. The Ag-*g*-HA/INS complex was formed.

Determination of the epoxy group content

The activated agarose solution (1 mL) was added to 10 mL of 0.5 mmol/L $Na_2S_2O_3$ (Guangzhou Chemical Reagent Factory) solution; this mixture was stirred and reacted [eq. (3)] for 0.5 h. The epoxy group content (mmol/g) of the activated agarose was determined by titration with 0.02 mol/L HCl:

$$C(\text{mmol/g}) = C_{\text{HCl}}(\text{mol/L}) \times V_{\text{HCl}}(\text{mL}) \times 10^{-3}/W(\text{g})$$

where C is the epoxy group content of the activated agarose, C_{HCl} is the concentration of HCl, V_{HCl} is the volume of HCl, and W is the weight of the activated agarose in a 1-mL solution:

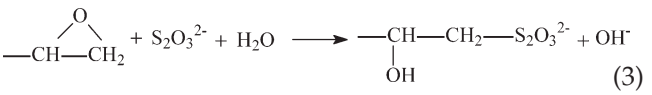

(3)

Characterization of Ag-*g*-HA

The viscosity of agarose with different degradation times was measured in water at 50°C by an Ubbelohde capillary viscometer (Guangzhou Zixin Chemicals Co., Guangzhou, China). The efflux time was recorded in triplicate, and the average viscosity of agarose was obtained. The relationship of the average viscosity ([η]) and the molecular weight of agarose (M) was determined by the classical Mark–Houwink equation[16]:

$$[\eta] = 1.40 \times 10^{-4} M^{0.83}$$

Because the molecular weight of the degraded agarose was positively related to its particle size in the solvent, the size dispersity of the degraded agarose was evaluated by a ζ sizer (Zeta Plus, Brookhaven Instruments Corporation, NY). Degraded agarose (1% w/w) was dissolved in hot water; then, 1 mL of the solution was added to 90 mL of ethanol with high speed stirring. The molecular weight dispersity of the degraded agarose was calculated according to its size dispersity.

The chemical structure of Ag-*g*-HA was checked by IR spectrometry (Equinox 55, Bruker Co., Germany) or element analysis (CHNS/O 2400, PerkinElmer, MA). IR spectrometry samples were prepared with IR-grade

potassium bromide in an agate mortar for KBr pellets. Elemental analysis of Ag-*g*-HA was performed on a PerkinElmer elementary analyzer.

Evaluation of the Ag-*g*-HA/INS microparticles

1. To determine the loading content and loading efficiency of INS, Ag-*g*-HA/INS microparticles were collected by ultracentrifugation at 15,000 rpm and 4°C for 30 min, and the concentration of free INS was assayed in the supernatant by high performance liquid chromatography (HPLC) (Agilent 1100, Agilent Technologies, Inc., Colorado). The drug-loading content and the loading efficiency of the Ag-g-HA/INS microparticles were determined according to the following equation[17,18]:

$$\text{Loading content}\,(\%) = \frac{\text{Total amount of insulin} - \text{Amount of free insulin}}{\text{Weight of complex}}$$

$$\text{Loading efficiency}\,(\%) = \frac{\text{Total amount of insulin} - \text{Amount of free insulin}}{\text{Total amount of insulin}}.$$

2. Atomic force microscopy analysis: 5 μL of an Ag-*g*-HA/INS microparticle suspension was dropped on a hydrophobic silica surface. After drying, the sample was rinsed in distilled water to remove salinity and then air-dried. The morphology of the Ag-*g*-HA/INS microparticles was observed under a Digital Instruments atomic force microscope (AutoProbe CP Researches, Thermomicroscopes, CA) in a tapping mode.
3. ζ sizer analysis: The size of the Ag-*g*-HA/INS microparticles was determined with a ζ sizer. The ζ potentials of Ag-*g*-HA in Tris buffer at different pH's (2.06, 3.16, 5.03, 6.5, and 7.35) were also detected by a ζ sizer.
4. *In vitro* release of INS: The release profile of INS from 10 mg of Ag-*g*-HA/INS microparticles was obtained in 10 mL of simulated physiological medium (pH's = 1.8, 6.8, and 7.4, to simulate gastrointestinal tract and bloodstream conditions) at 37°C under agitation (100 rpm). At certain intervals, 1 mL of solution from the medium was taken out for INS content analysis by HPLC; in the meantime, 1 mL of buffer was compensated into the medium. The release kinetics of Ag-*g*-HA/INS in different pH environments was examined by the Weibull distribution.

RESULTS AND DISCUSSION

Degradation of agarose

Agarose might be easily degraded by enzymes, hydrogen peroxide, or other oxidants. For convenience, hydrogen peroxide is the best choice for the degradation of agarose because of the high cost of agarose and difficult disposal of other oxidants. Figure 1 shows that the viscosity-average molecular weights of agarose changed with degradation time. This indicated that the molecular weight of agarose continuously decreased with degradation time over 13 h and then was constant after 13 h. The result of ζ sizer analysis (Table I) showed that the molecular weight dispersity of the degraded agarose with degradation times of 5 or 6 h was small; for example, it was between 43 and 60 kDa for 5 h of degradation and between 35 and 51 kDa for 6 h of degradation. After agarose was degraded for 5 or 6 h, the gelling temperature of the agarose was 37 or 28°C, respectively. However, agarose degraded for 13 h or more did not form a gel at room temperature for a certain time. These results indicate that the lower molecular weight was, the lower gelling temperature was. Generally, copolymers with a gelling temperature below body temperature can improve their encapsulating efficiency.[19] Therefore, in this study, we chose the agarose degraded for 6 h to synthesize the Ag-*g*-HA copolymer with a relative low gelling temperature for INS loading.

Reaction of agarose with epichlorohydrin

Compared to other reacting agents, epichlorohydrin has a higher activation and lower toxicity and is widely useful in polymer modifications[20–22] and crosslinking reactions.[23–25] By titration analysis, it was known that the epoxy group content of agarose was 1.55 mmol/g after the degraded agarose was reacted with epichlorohydrin for 5 h. Meanwhile, part of the final products were water-insoluble; this may have been due to the ring-opening reaction of the epoxy group and the self-crosslinking with hydroxyl groups in agarose. When the reacting process was shortened to 3 h, most of the final products were water-soluble.

Evidence for grafting

The Fourier transform infrared (FTIR) spectra of HA and Ag-*g*-HA are shown in Figure 2. The FTIR

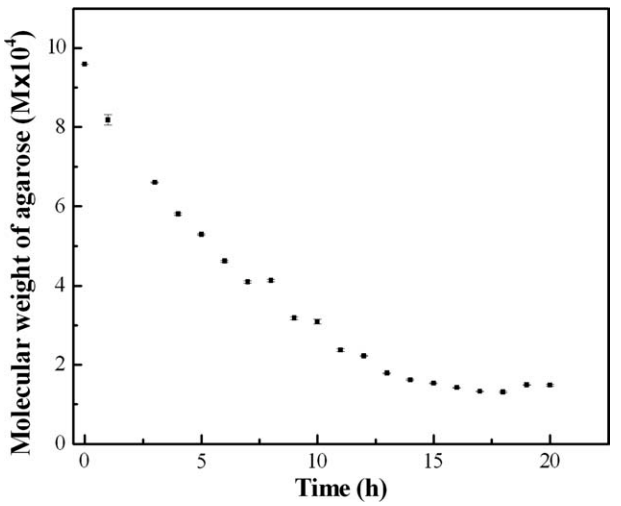

Figure 1 Effect of the degradation time on the molecular weight of agarose. Reaction conditions: agarose concentration = 2% (w/w), H_2O_2 concentration = 2% (v/v), and temperature = 55°C.

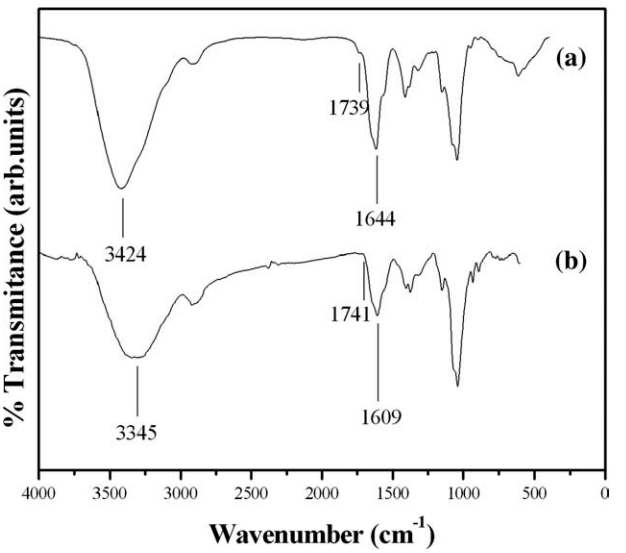

Figure 2 IR spectra of (a) HA and (b) Ag-*g*-HA.

spectrum of HA showed a strong O—H stretching vibration band at 3424 cm^{-1}, an absorption band of C=O stretching vibrations of carboxyl groups at 1739 cm^{-1}, and a band of C=O stretching vibrations of the secondary amide (amide I band) at 1644 cm^{-1}. In the FTIR spectrum of Ag-*g*-HA, the peak of O—H stretching vibrations shifted to 3345 cm^{-1} and was responsible for the grafting reaction of HA and weakened due to the decrease of hydroxyl groups; meanwhile, the existence of absorption bands of the secondary amide at 1609 cm^{-1} also indicated that HA was grafted onto the agarose chain.

The reaction product was divided into two parts: one was in the supernatant phase (dissolved), and the other was in the precipitation phase because of additional crosslinking during grafting. The elemental analysis data of these products are presented in Table II. The N content of Ag-*g*-HA forming the supernatant phase was 2.57%, whereas that in the precipitate phase was 2.11%. Compared to the N content of HA, 3.87%, the calculated grafting ratio of Ag-*g*-HA was about 66.41% for the product from the supernatant phase and 54.52% for the product from the precipitation one, respectively. In this study, we used Ag-*g*-HA from the supernatant as an INS carrier.

TABLE I
Dispersity of the Particle Size (nm) of Agarose Degraded for 5 or 6 h

Agarose degradation time	Maximal size	Minimal size	Average size
5 h	411.32	157.92	282.5
6 h	164.62	54.18	124.68

Ag-*g*-HA/INS microparticles

Ag-*g*-HA and INS were able to form an approximate spherical shape via electrostatic interaction between INS and HA and by the gelling effect of agarose. As illustrated in Figure 3, Ag-*g*-HA/INS complexes appeared to be spherical with a size of about 2–10 μm. Meanwhile, the results of ζ sizer analysis also showed the INS-loaded complex with an average particle size of 2 μm. The FTIR spectra of INS and Ag-*g*-HA/INS are shown in Figure 4. In the IR spectrum of INS, an absorption band appearing at 1657 cm^{-1} corresponded to the C=O stretching vibration of the amide I, and the peak at 1540 cm^{-1} corresponded to the amide II peak. In the IR spectrum of Ag-*g*-HA/INS, the absorption band of HA at 1739 cm^{-1} in Figure 2(a) became weak after INS was loaded, and the amide II peak of INS at 1540 cm^{-1} disappeared or shifted. This evidence indicated the formation of polyanionic–polycationtic Ag-*g*-HA/INS complexes.

The particle sizes of human growth hormone[26] or INS complexing with HA[27] developed earlier by other investigators were small and formed a totally transparent solution. In the same process of Ag-*g*-HA copolymer composite formation with INS, the sizes of the particles were about few micrometers. These facts could be explained with the mechanism

TABLE II
Elemental Analysis Data of Ag-*g*-HA and Agarose

Sample	C (%)	H (%)	N (%)
Supernatant of Ag-*g*-HA	39.03	6.67	2.57
Supernatant of control	38.97	7.25	0.56
Precipitate of Ag-*g*-HA	40.64	7.42	2.11
Precipitate of control	40.81	7.55	0.20
Agarose	41.93	7.0	−0.42

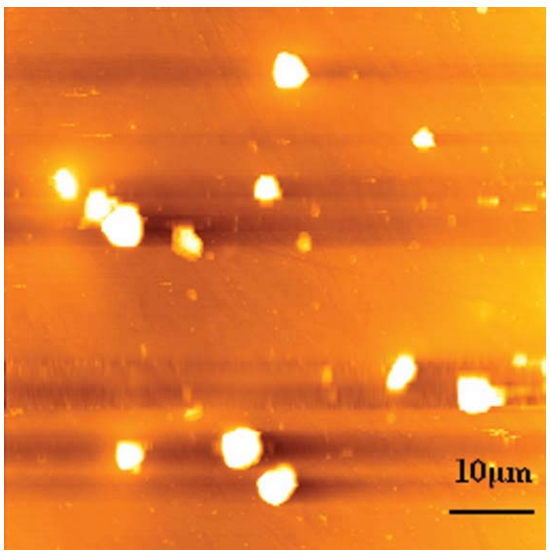

Figure 3 Atomic force microscopy morphologies of the Ag-*g*-HA/INS microparticles. [Color figure can be viewed in the online issue, which is available at www.interscience.wiley.com.]

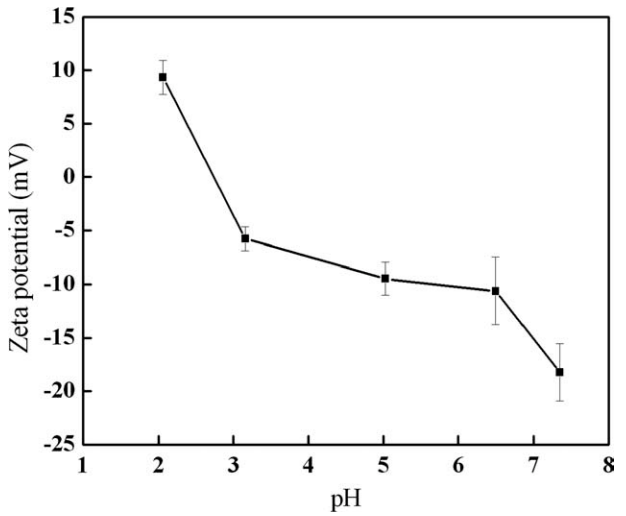

Figure 5 ζ potentials of Ag-*g*-HA in Tris buffer with different pH's.

of complex formation that Jederstrom et al.[27] deduced. Electrostatic interactions contributed to the formation of the complex between Ag-*g*-HA and INS. During the dialysis process, the dissociation of free carboxyl groups of HA in the complex made the complex become negative with increasing pH values above 3 (Fig. 5); this was indicated in the ζ sizer measurement results. The presence of anionic carboxylic groups led to a loose Ag-*g*-HA chain; this resulted from electrostatic repulsion, which favored the interaction of Ag-*g*-HA with INS, which carried opposite charges. Meanwhile, the charge of INS remained positive when the pH of medium was less than its isoelectric point (pH 5.4). On the other hand, the INS molecule bore a lower net charge during dialysis; this resulted from the dissociation of the carboxyl groups of INS with increasing pH value to 5.4. The reduction of net charge decreased the double layer according to the DLVO theory (Theory of colloid flocculation advanced independently by Derjaguin and Landau, Verwey and Overbeek),[28,29] and increased the hydrophobic interactions of INS and Ag-*g*-HA. Thus, when pH value increased above 3 and the concentration of electrolytes was lowered further, the repulsive energy potential between INS and HA caused by the diffuse double layer decreased, and the attractive energy potential dominated over the repulsive one. In this situation, a complex between Ag-*g*-HA and INS could actually be formed when the ionic strength was low. Figure 6 shows the INS loading efficiency or loading

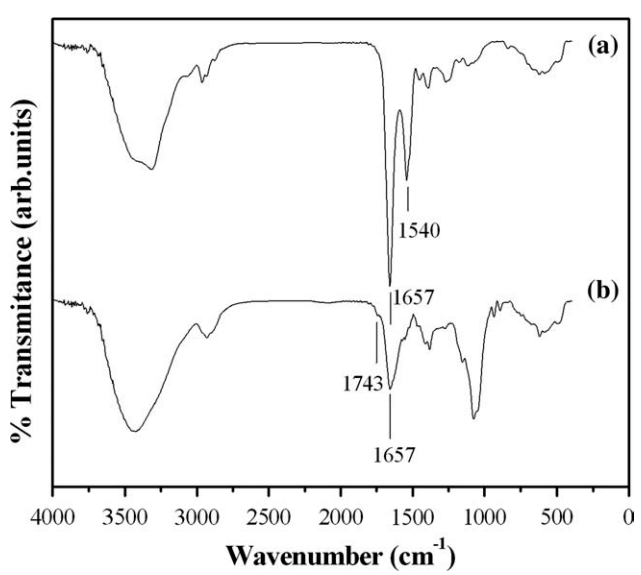

Figure 4 IR spectra of (a) INS and (b) Ag-*g*-HA/INS.

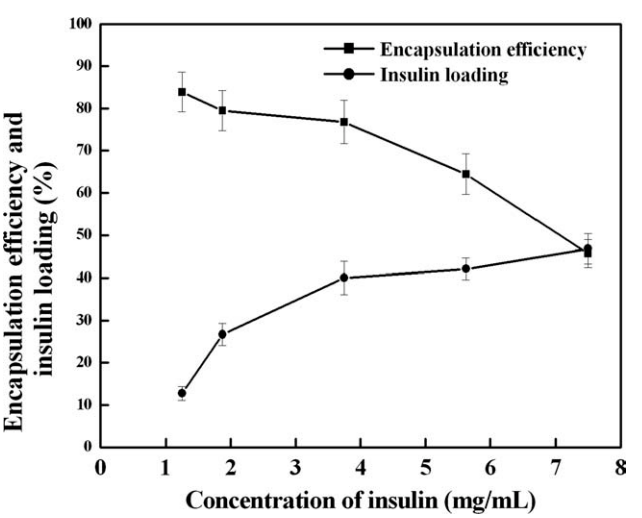

Figure 6 Effect of the INS concentration on the encapsulation efficiency and INS loading of Ag-*g*-HA.

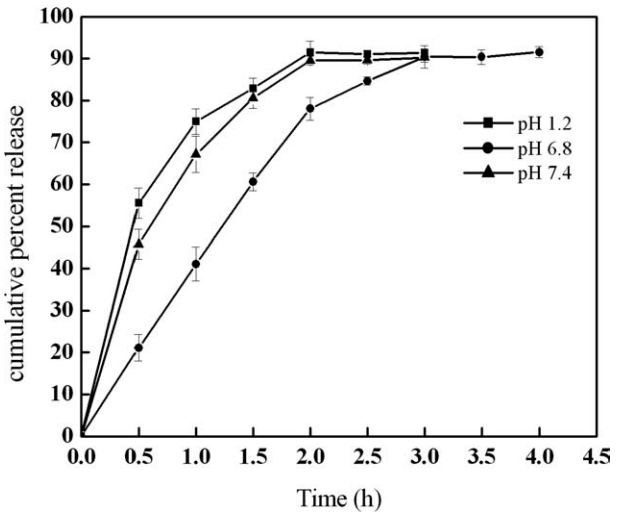

Figure 7 Release profiles of INS from the Ag-*g*-HA/INS microparticles in different pH environments at 37°C.

content (76.8 ± 5.1 or 40.04 ± 3.9%, respectively) obtained with an INS concentration of 3.75 mg/mL.

Release behavior of the Ag-*g*-HA/INS microparticles

Figure 7 shows the release profiles of INS from the Ag-*g*-HA/INS microparticles at pH values of 1.2, 6.8, and 7.4 for simulation of the pH environment of the stomach after a meal, the intestine, and the bloodstream, respectively. At pH 1.2 or 7.4, a significant burst release effect was observed at the initial stage (30 min), and the cumulative amount of release reached 50.55 ± 3.61 and 45.75 ± 3.57%, respectively. The release process finished within 2 h. However, at pH 6.8, the amount of release was 21.11 ± 3.15% during the first 30 min, which showed a slower release rate, and a complete release was realized within 3 h. Ag-*g*-HA//INS microparticles were formed via electrostatic interaction at pH 3–5.4, which resulted from the charge change of the components in the complexes with the variation of the pH value. In pH 1.2 medium, the undissociated carboxylic groups and high content of protonated amino groups of Ag-*g*-HA led to a net positive charge (the ζ potential of Ag-*g*-HA at pH 2.06 was 9.34 ± 1.59 mV), and the aggregation of Ag-*g*-HA chain was loose. Meanwhile, INS bore positive charges. The electrostatic repulsion between Ag-*g*-HA and INS provoked the instability of Ag-*g*-HA/INS microparticles and caused a quick release of INS. On the contrary, in pH 7.4 medium (above the isoelectric point of INS), INS bore negative charges, which resulted from the highly dissociated carboxylic groups (the ζ potential of Ag-*g*-HA at pH 7.35 was −18.22 ± 2.68 mV), and the electrostatic repulsive force between INS and Ag-*g*-HA also led INS to release quickly. In pH 6.8 medium, there was less electrostatic repulsion between fewer negative charges of Ag-*g*-HA (the ζ potential of Ag-*g*-HA at pH 6.5 was −10.61 ± 3.13 mV) and INS, which might have been responsible for the slower release of INS. These results prove that the stability of the complexes in different pH environments significantly affected their INS release. A significant sustained-release behavior at pH 6.8 or 7.4 would be expected if a basic peptide was combined with Ag-*g*-HA instead of INS because the formed complex of a basic peptide and Ag-*g*-HA would be more stable in these pH media. From these results, we suggest that it is necessary to coat peptide complexes with enteric material to avoid drug delivery in the stomach and target drug to the intestinal region. We expect that HA as a CD44 receptor, has a mucoadhesive feature,[30] which may aid in its application as a potential targeted delivery vehicle for drugs to the gastrointestinal tract[31,32] and improve the drug bioavailability and effectiveness.

The release profiles were described by the empirical Weibull function[33]:

$$F(t) = 1 - \exp[-(t^b/a)] \tag{4}$$

where $F(t)$ is the fraction of the total drug released at time t, a is scale parameter of the microparticles, and b is a shape parameter of microparticles. Equation (4) may be rearranged into the following:

$$\ln\{\ln[1/1 - F(t)]\} = b \ln t - \ln a \tag{5}$$

This equation fits almost all kinds of release systems because of its independence from the geometry of the delivery device or particle. The release data of the Ag-*g*-HA/INS microparticles was fitted to the Weibull function. Table III summarizes the results of the regression analyses. The parameters of the Weibull equation, scale (a) and shape (b), are related to r^2 (correlation coefficient). The r was near 1, which meant that the release behavior of the Ag-*g*-HA/INS microparticles fit these equations. The value of b for Ag-*g*-HA/INS at pH 6.8 was higher than at pH 1.2 or 7.4. Moreover, a at pH 1.2 or 7.4 was positive, whereas at pH 6.8, it was negative. This difference showed that the pH influenced the drug release from the Ag-*g*-HA//INS microparticles.

TABLE III
Estimates of the Weibull Parameters for the AG-*g*-HA/INS Microparticles

pH	a	b	r^2
1.2	0.2971	0.655	0.9586
6.8	−1.2488	1.9301	1
7.4	0.1116	0.7927	0.9656

CONCLUSIONS

Agarose with different molecular weights was readily obtained by hydrogen peroxide degradation. After it was activated by epichlorohydrin, agarose was easily connected with HA. The formation of the Ag-*g*-HA copolymer was confirmed by IR spectroscopy and elemental analysis. Ag-*g*-HA and INS were able to form polyelectrolyte complexes via electrostatic interaction at pH 3–5.4. *In vitro* drug-release experiments proved that the Ag-*g*-HA/INS microparticles had a burst release effect at pH 1.2 and 7.4, but the release behavior was ideal in the environment at pH 6.8. The release data was fitted to the Weibull equation. These results demonstrate that the Ag-*g*-HA copolymer possesses potential as a peptide carrier.

The authors thank the Key Lab of Biomaterials, Guangdong Education Committee, for the free use of some instruments and equipment.

References

1. Chen, H.; Yan, X.; Zhu, P.; Lin, J. Nutr J 2006, 5, 31.
2. Tang, S. Q.; Yang, W.; Mao, X. Biomed Mater 2007, 2, 2.
3. Lee, J. B.; Hayashi, K.; Hirata, M.; Kuroda, E.; Suzuki, E.; Kubo, Y.; Hayashi, T. Biol Pharm Bull 2006, 29, 2135.
4. Aruffo, A.; Stamenkovic, I.; Melnik, M.; Underhill, C. B.; Seed, B. Cell 1990, 61, 1303.
5. Gustafson, S.; Bjorkman, T.; Westlin, J. E. Glycoconjugate J 1994, 99, 608.
6. Yi, L.; Glenn, D. P. Bioconjugate Chem 1999, 10, 755.
7. Yi, L.; Michael, R. Z.; Glenn, D. P. Biomacromolecules 2000, 1, 208.
8. Charlot, A.; Heyraud, A.; Guenot, P.; Rinaudo, M.; Auzely-Velty, R. Biomacromolecules 2006, 7, 907.
9. Peattie, R. A.; Nayate, A. P.; Firpo, M. A.; Shelby, J.; Fisher, R. J.; Prestwich, G. D. Biomaterials 2004, 25, 2789.
10. Cai, S.; Liu, Y.; Zheng, S. X.; Prestwich, G. D. Biomaterials 2005, 26, 6054.
11. Kazuteru, M.; Tooru, O.; Nobuhiko, Y. J. Controlled Release 1999, 59, 77.
12. Anthony, J. D.; John, K. S. Carbohydr Glycoconjugates 2001, 99, 617.
13. Ghosh, I.; Chattopadhaya, R.; Kumar, V.; Chakravarty, B. N.; Datta, K. Soc Reprod Fertil Suppl 2007, 63, 539.
14. Hang, S. K.; Lee, J. H.; Kim, D.; Cho, S. H.; Yuk, S. H. Sci Tech Adv Mater 2005, 6, 468.
15. Seyfried, N. T.; Mcvey, G. F.; Almond, A.; Mahoney, D. J.; Dudhia, J.; Day, A. J. J Biol Chem 2005, 280, 5435.
16. Knaul, J. Z.; Kasaai, M. R.; Bui, V. T.; Creber, K. A. Can J Chem 1998, 76, 1699.
17. Grenha, A.; Sejjo, B.; Remunan-Lopez, C. Eur J Pharm Sci 2005, 25, 427.
18. Lin, Y. H.; Mi, F. L.; Chen, C. T.; Chang, W. C.; Peng, S. F.; Liang, H. F.; Sung, H. W. Biomacromolecules 2007, 8, 146.
19. Attwood, D.; Zhou, Z.; Booth, C. Expert Opin Drug Deliv 2007, 4, 533.
20. Costa, S. A.; Reis, R. L. J Mater Sci Mater Med 2004, 15, 335.
21. Mehta, A.; Zydney, A. L. J Membr Sci 2008, 313, 304.
22. Liu, Z. T.; Yang, Y. N.; Zhang, L. L.; Sun, P.; Liu, Z. W.; Lu, J.; Xiong, H.; Peng, Y.; Tang, S. Carbohydr Polym 2008, 71, 18.
23. Porath, J.; Janson, J. C.; Loos, T. J Chromatogr 1971, 60, 167.
24. Starr, B.; Burts, E.; Upson, J. R.; Riffle, J. S. Polymer 2001, 42, 8727.
25. Simkovic, I.; Hricovini, M.; Soltes, L.; Mendichi, R; Cosentino, C. Carbohydr Polym 2000, 41, 9.
26. Jederstrom, G. U.S. Pat. 6,448,093 (2002).
27. Jederstrom, G.; Andersson, A.; Grasjo, J.; Sjoholm, I. Pharm Res 2004, 99, 2040.
28. Derjaguin, B. V.; Abricosova, I. L.; Lifshitz, E. M. Q. Rev Chem Soc 1956, 10, 295.
29. Derjaguin, B. V. Sci Am 1960, 203, 47.
30. Sigurdsson, H. H.; Loftsson, T.; Lehr, C. M. Int J Pharm 2006, 325, 75.
31. Si-Tahar, M.; Sitaraman, S.; Shibahara, T.; Madara, J. L. Am J Physiol Cell Physiol 2001, 280, C423.
32. Reid, S. D.; Pockley, A. G. Immunol Invest 2000, 29, 271.
33. Langenbucher, F. K. J Pharm Pharmacol 1972, 24, 979.